AFGL-TR-76-0240
ENVIRONMENTAL RESEARCH PAPERS, NO. 579

# Nitrogen Dioxide Absorption Coefficients at High Temperatures

D. E. PAULSEN
R. E. HUFFMAN



5 October 1976



This research was sponsored by the Defense Nuclear Agency under Subtask S99QAXHI002, Work Unit 30.

AERONOMY DIVISION PROJECT CDNA
AIR FORCE GEOPHYSICS LABORATORY
HANSCOM AFB, MASSACHUSETTS 01731

AIR FORCE SYSTEMS COMMAND, USAF

This technical report has been reviewed and
is approved for publication.

FOR THE COMMANDER

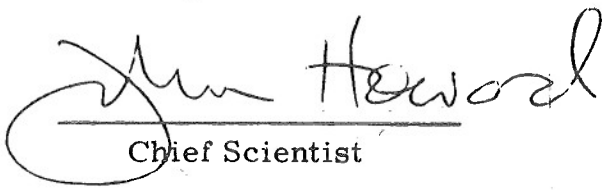

Chief Scientist

Qualified requestors may obtain additional copies from the Defense Documentation Center. All others should apply to the National Technical Information Service.

Unclassified

SECURITY CLASSIFICATION OF THIS PAGE *(When Date Entered)*

| REPORT DOCUMENTATION PAGE | | READ INSTRUCTIONS BEFORE COMPLETING FORM |
|---|---|---|
| 1. REPORT NUMBER<br>AFGL-TR-76-0240 | 2. GOVT ACCESSION NO. | 3. RECIPIENT'S CATALOG NUMBER |
| 4. TITLE *(and Subtitle)*<br>NITROGEN DIOXIDE ABSORPTION COEFFICIENTS AT HIGH TEMPERATURES | | 5. TYPE OF REPORT & PERIOD COVERED<br>Scientific<br>6. PERFORMING ORG. REPORT NUMBER<br>ERP No. 579 |
| 7. AUTHOR(s)<br>D.E. Paulsen<br>R.E. Huffman | | 8. CONTRACT OR GRANT NUMBER(s) |
| 9. PERFORMING ORGANIZATION NAME AND ADDRESS<br>Air Force Geophysics Laboratory (LK)<br>Hanscom AFB<br>Massachusetts 01731 | | 10. PROGRAM ELEMENT, PROJECT, TASK AREA & WORK UNIT NUMBERS<br>62704H<br>CDNA0003 |
| 11. CONTROLLING OFFICE NAME AND ADDRESS<br>Air Force Geophysics Laboratory (LK)<br>Hanscom AFB,<br>Massachusetts 01731 | | 12. REPORT DATE<br>5 October 1976<br>13. NUMBER OF PAGES<br>28 |
| 14. MONITORING AGENCY NAME & ADDRESS*(If different from Controlling Office)* | | 15. SECURITY CLASS. *(of this report)*<br>Unclassified<br>15a. DECLASSIFICATION/DOWNGRADING SCHEDULE |

16. DISTRIBUTION STATEMENT *(of this Report)*

Approved for public release; distribution unlimited.

17. DISTRIBUTION STATEMENT *(of the abstract entered in Block 20, if different from Report)*

18. SUPPLEMENTARY NOTES

This research was sponsored by the Defense Nuclear Agency under Subtask S99QAXHI002, Work Unit 30.

19. KEY WORDS *(Continue on reverse side if necessary and identify by block number)*

Nitrogen dioxide
Absorption coefficients
High temperature

20. ABSTRACT *(Continue on reverse side if necessary and identify by block number)*

The absorption coefficient of nitrogen dioxide, $NO_2$, is used in models of the fireball resulting from atmospheric nuclear detonations. This report gives values for the absorption coefficient obtained at wavelengths between 380 and 760 nm and at temperatures between 669 and 1313°K. The absorption coefficient varies from a maximum of about 10 $cm^{-1}$ near 400 nm to about 0.1 $cm^{-1}$ at the longest wavelength observed. The results agree with previously published data, which were available for only a few wavelengths, and provide a

DD FORM 1 JAN 73 1473 EDITION OF 1 NOV 65 IS OBSOLETE

Unclassified

SECURITY CLASSIFICATION OF THIS PAGE *(When Date Entered)*

20. (Cont)

comprehensive data set over the temperature and wavelength regions studied. Comparison of these results is made with $NO_2$ thermal emission intensities.

## Contents



## Illustrations

## Illustrations



## Tables

# Nitrogen Dioxide Absorption Coefficients at High Temperatures

## I. INTRODUCTION

In 1970, Paulsen, Sheridan, and Huffman published data on the spectral radiant intensity of thermally excited nitrogen dioxide, $NO_2$.[1*] The measurements, which covered the wavelength region from 460 to 860 nm and the temperature region from 972 to 1335°K, were useful in problems concerned with radiative transport in hot air. Since the measurements are more detailed in wavelength and temperature than published high temperature absorption coefficients,[2] there is a natural tendency to use the emission intensities[1,3] to calculate absorption coefficients. When this is done, however, the calculated absorption coefficients show a marked deviation from the measured absorption coefficients[2-11] as shown in Figure 1. The higher temperature measurements are obtained in part from shock tube data at a few isolated wavelengths and are estimated to have experimental uncertainties on the order of 10 percent.

(Received for publication 4 October 1976)

*Because of the large number of references mentioned in the above text, please refer to Reference Page No. 23 for References 1 through 11.

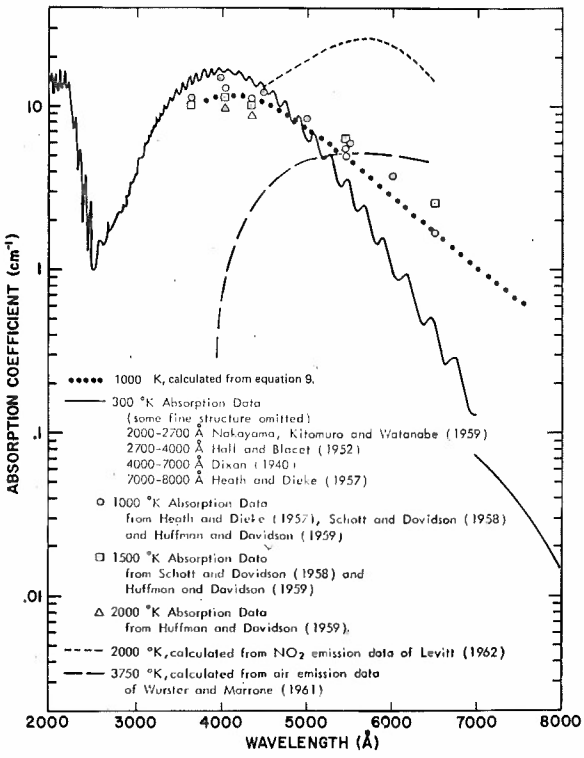


Figure 1. Absorption Coefficients for $NO_2$ at Various Temperatures and Wavelengths (From Reference 2, in part)

These absorption coefficients at elevated temperatures are of interest because of the importance of $NO_2$ as an emitter in high-temperature air.[2] One situation occurs in the lower temperature ranges of the fireball created by atmospheric nuclear detonations. The computer codes used to predict the air opacity and other properties of the highly perturbed atmospheric region resulting from the nuclear detonation require absorption coefficients, or cross-sections, for the absorption of photons by $NO_2$ and the other constituents of the fireball.

We have obtained $NO_2$ absorption coefficients in conjunction with our earlier study[1] of emission from hot $NO_2$. Although the temperature range is not as high as desirable for some uses, the measurements have proved to be of interest to others in connection with fireball models. We are therefore making these absorption coefficients more readily available by the publication of this report.

## 2. EXPERIMENTAL

Much of the equipment used for these measurements is described in detail in the earlier paper.[1] The major change was the design of the cell. Figure 2 shows the experimental arrangement. The quartz absorption cell was heated with an

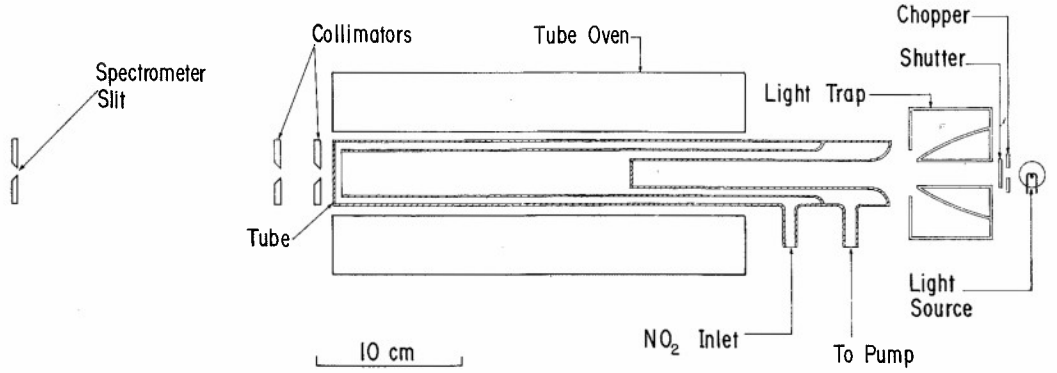


Figure 2. Schematic of High Temperature Absorption Apparatus. The collimators are of cylindrical geometry and are placed so that radiation from the side walls of the cell cannot enter the spectrometer. The entire system was covered to eliminate ambient radiation. Absorption tube was made of quartz

electric tube oven. The cell was designed so that both windows were well within the oven to minimize thermal gradients along the absorption path length. Gas pressures were measured outside the oven with a Pace KP-15 pressure transducer which was calibrated against a mercury manometer. Temperatures were measured with a chromel-alumel thermocouple in good thermal contact with the outside of the cell. A tungsten filament, powered by a current-regulated supply, was used for the light source. The source radiation, which was chopped at 400 Hz with an American Time Products tuning fork chopper, passed through the light trap, the absorption cell, and a series of collimating baffles into the entrance slit of a Spex 3/4 m Czerny-Turner spectrometer, Model 1600. Measurements were made with both slits at 200 $\mu$m, which corresponds to a calculated bandwidth of 0.22 nanometers. An EMI 9558 photomultiplier tube was used as the sensor. The photocurrent was amplified by a PAR lock-in amplifier, Model HR-8, and recorded.

Nitrogen dioxide, $NO_2$, purified by repeated freezing and pumping until no trace of color (blue-green) could be observed in the white solid, was admitted to the heated cell until the desired pressure was reached. The $NO_2$ supply was then shut off. Approximately 2 min were necessary to achieve a steady state, as evidenced by variation in the photocurrent due to absorption by the $NO_2$. After equilibration, a spectral scan of several tens of nanometers was recorded along with the pressure and the thermocouple readings. Each absorption scan was bracketed by similar scans with the cell evacuated to provide the reference photocurrents. In this manner absorption measurements were made at wavelengths from 380 to 760 nm and at temperatures from 669 to 1313 °K.

## 3. RESULTS

The first step in reducing the data is to determine the pressure of $NO_2$ in the oven. Assuming that the gas in the oven was at thermodynamic equilibrium, the mole fraction of $NO_2$ was calculated from the equilibrium constant for the dissociation of $NO_2$ into NO and $O_2$, which is obtained from thermodynamic quantities listed in the JANAF Thermochemical Tables.[12] The $2\ NO_2 \rightleftarrows N_2O_4$ equilibrium is not significant at these temperatures. Absorption coefficients at 10-nm intervals are then calculated using the relation

$$k = \frac{760\ T}{(273)\ P\ell}\ \ell n \frac{I_o}{I} \tag{1}$$

where k is in units of $cm^{-1}$, T is in °K, P is the calculated $NO_2$ pressure, and $\ell$ is the cell length (20.0 cm).

Preliminary results indicated that k had a significant pressure dependence. Absorption coefficients at high system pressures, near 760 torr, were reasonably constant, but as the system pressure was lowered below about 300 torr an increase in the absorption coefficient was observed. The effect is attributed to the fact that the closed system is partly at oven temperature and partly at room temperature. The dissociation equilibrium

$$2NO_2 \underset{k_b}{\overset{k_f}{\rightleftarrows}} 2NO + O_2$$

is shifted far to the right at oven temperatures and far to the left at room temperature, thus creating a situation where the $NO_2$ outside of the oven tends to diffuse into the oven while the NO and $O_2$ inside the oven tend to diffuse out.

To aid in understanding this effect, data were taken at selected wavelengths and temperatures over a large range in pressures. A typical set of data is shown in Figure 3, where log k, as calculated by Eq. (1), is plotted against log $P_{System}$ with T = 896°K and $\lambda$ = 600 nm. In making these measurements it was obvious that a steady state was attained within a few minutes. Therefore, we write the steady state approximation for the pressure of $NO_2$ in the oven

$$\frac{d(P_{NO_2})}{dt} = 0 \cong -k_f (P_{NO_2})^2 + k_b (P_{NO})_o^2 (P_{O_2})_o + D (P_{NO_2})_a \tag{2}$$

12. JANAF Thermochemical Tables, (1965) Dow Chemical, Midland, Michigan.

where subscript o indicates oven and subscript a indicates ambient temperature, and the last term is the perturbation of equilibrium by diffusion of $NO_2$ into the oven. Because of their large partial pressures, diffusion of NO and $O_2$ out of the oven will be less significant.

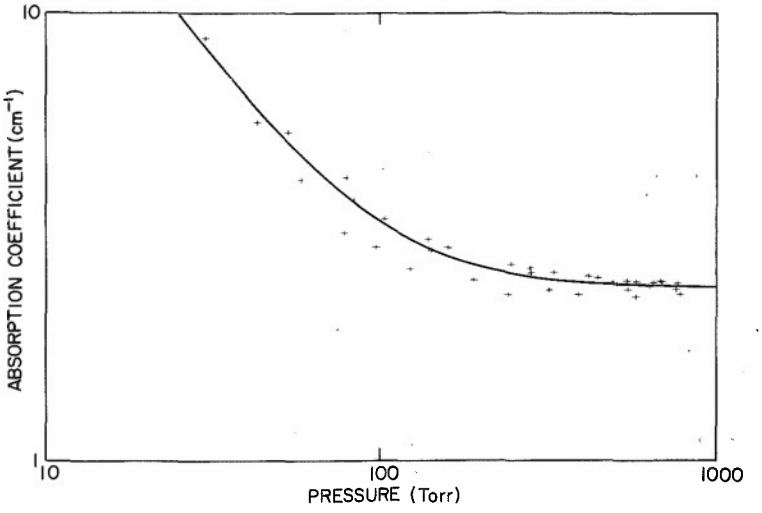


Figure 3. Apparent Absorption Coefficients at 600 Nanometers and 896°K as a Function of System Pressure. The variation in absorption coefficient appears to be due to diffusion of cold $NO_2$ into the absorption cell as explained in the text. The curve represents a linear regression fit of Eq. (7), the coefficients are shown in Table 1

Equation (2) may be rearranged as

$$(P_{NO_2})_o = \left[\frac{k_b (P_{NO})_o^2 (P_{O_2})_o}{k_f}\right]^{1/2} \left[1 + \frac{D(P_{NO_2})_a}{k_b (P_{NO})_o^2 (P_{O_2})_o}\right]^{1/2}. \quad (3)$$

Although the small partial pressure of $NO_2$ in the oven may change drastically, the percentage effect on NO and $O_2$ is considerably less. Therefore, it is assumed that the second factor is a perturbation on the equilibrium and that Eq. (3) can be approximated by

$$(P_{NO_2}) = (P'_{NO_2})_o \left\{ 1 + \frac{D(P_{NO_2})_a}{k_b (P_{NO})_o^2 (P_{O_2})_o} \right\}^{1/2}$$

$$\cong (P'_{NO_2}) \left\{ 1 + \frac{2D(1 + \frac{\alpha}{2})^3}{k_b \alpha^3 P_t^2} \right\}^{1/2} . \quad (4)$$

Ignoring the relatively minor variation of the $(1 + \frac{\alpha}{2})$ factor gives

$$(P_{NO_2})_o \cong (P'_{NO_2})_o \left\{ 1 + \frac{\beta}{\alpha^3 P_t^2} \right\}^{1/2} \quad (5)$$

where $(P'_{NO_2})_o$ is the calculated pressure in the absence of the diffusive perturbation, and $\alpha$ is the fractional dissociation of $NO_2$. Equation (1) is rewritten

$$k_{app} = \frac{760}{273} \frac{T}{(P'_{NO_2})_o \ell} \ln \frac{I_o}{I}$$

where $k_{app}$ is the apparent absorption coefficient based on $(P'_{NO_2})_o$.

It follows that

$$k_{app} (P'_{NO_2})_o = k (P_{NO_2})_o$$

and

$$k_{app} \sim k \left\{ 1 + \frac{\beta}{\alpha^3 P_t^2} \right\}^{1/2} \quad (6)$$

where k is the actual absorption coefficient. The data in Figure 3 were fitted to the relation

$$k_{app}^2 = k^2 + \frac{\beta k^2}{\alpha^3 P_t^2} \quad (7)$$

by linear regression. The quality of the fit is shown by the smooth line in Figure 3. Equation (7) was fitted to sets of data obtained at the temperatures and wavelengths shown in Table 1. The results are tabulated in Table 1 and shown in Figure 4.

For interpolation purposes $\ell n\ \beta$ values were fitted to a quartic in $10^3/T$, which is shown by the smooth curve in Figure 4 and given by

$$\ell n\ \beta = -16.168528 + 24.218754(10^3/T) - 11.448829(10^3/T)^2 - 2.050242(10^3/T)^3 + 1.281069(10^3/T)^4.$$

This interpolation formula gives excellent results over the range of experimental data and appears to give reasonable values for minor extrapolations. The variation of $\beta$ with T is not explained here. However, as derived above, $\beta$ is proportional to a diffusion coefficient and inversely proportional to a reaction rate constant. It is possible that the perturbing effect of diffusion is overcome at higher temperatures by faster reactions.

Table 1. Coefficients of Eq. (7) for Various Temperatures and Wavelengths

| T(°K) | λ(nm) | $\beta(atm^2)$ | $k(cm^{-1})$ |
|---|---|---|---|
| 669 | 640 | $2.47\times10^{-3}$ | 0.967 |
| 763 | 600 | $7.29\times10^{-3}$ | 1.95 |
| 828 | 600 | $1.08\times10^{-2}$ | 2.23 |
| 893 | 600 | $1.41\times10^{-2}$ | 2.44 |
| 980 | 420 | $1.58\times10^{-2}$ | 11.41 |
| 1083 | 600 | $1.39\times10^{-2}$ | 3.10 |
| 1206 | 500 | $1.10\times10^{-2}$ | 7.54 |
| 1315 | 420 | $7.82\times10^{-3}$ | 11.25 |

The true absorption coefficient, k, is obtained from

$$k = \frac{760\ T}{273\ (P'_{NO_2})\ \ell\ (1 + \beta/\alpha^3 P_t^2)^{1/2}}\ \ell n\ \frac{I_o}{I}. \qquad (8)$$

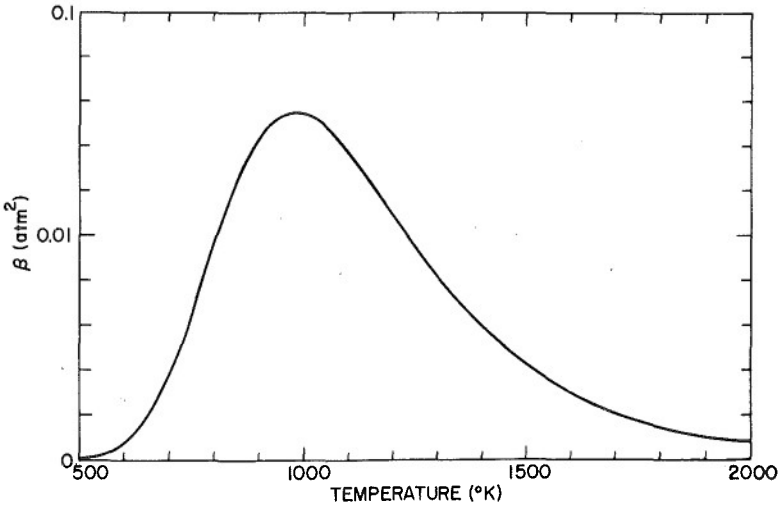


Figure 4. Variation of the Coefficient $\beta$ of Eq. (7) With Temperature. The curve represents the equation in the text

To illustrate the effectiveness of this correction for diffusion, absorption coefficients were calculated by Eq. (8) for the data which is summarized in Table 1. In order to show the results in a single plot (Figure 5) the data is presented as the percent deviation of k calculated from Eq. (8) and the corresponding value of k, the square root of the intercept of Eq. (7). For the data in Table 1, 20 to 40 different pressures were utilized. The data points are clustered quite tightly at the higher pressures and show more scatter, as would be expected, at lower pressures. The standard deviation of the data shown in Figure 5 is 5.1 percent.

Equation (8) is then used to calculate the absorption coefficients from the larger block of data taken at 10-nm intervals from the absorption scans. The data were obtained at eight temperatures ranging from 669 to 1313°K and over wavelengths ranging from 380 to 760 nanometers. Absorption scans were made at two distinct pressures at each temperature. This resulted in two absorption coefficients at each temperature and selected wavelengths in the regions without overlap, and four absorption coefficients at each temperature and wavelength where there was overlap. In one case, 1317°K and 720 to 760 nm, there was only one absorption scan. To simplify presentation of the data, Tables 2a and 2b list, at each temperature and wavelength, the mean absorption coefficient, the standard deviation, and the number of data points. The data are also shown in Figures 6 through 13, where each measured absorption coefficient is plotted as a function of wavelength for a specific temperature. The smooth curves in the figures are given by the equation

$$k = k_{max} \exp \left[ -1481.3(\Delta E)^2/T \right] \text{ cm}^{-1} \qquad (9)$$

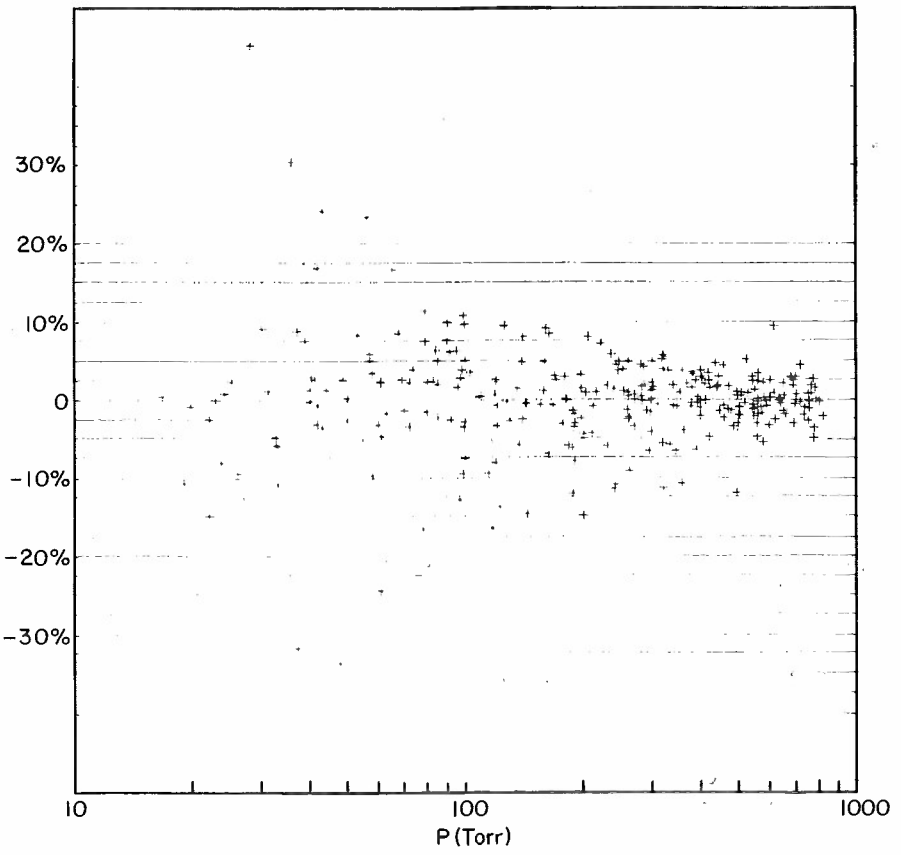


Figure 5. Scatter of Absorption Coefficient Data as a Function of System Pressure. Table 1 data only

where $k_{max}$ = absorption coefficient at $\lambda_{max}$

$$= \left[ \frac{14.84 + 214.3 \exp(-3267/T)}{Q_v} \right] \quad cm^{-1}$$

$$\Delta E = \left[ E_{max} - E_{\lambda} \right] \quad eV$$

$E_{max}$ = $E_{\lambda}$ at $\lambda_{max}$

$$= 3.04 \text{ eV}$$

$$E_{\lambda} = \left[ 1239.85/\lambda \right] \quad eV \quad (\lambda \text{ in nm})$$

and

$$Q_v = \text{vibrational partition function for } NO_2$$

$$= \prod_{i=1}^{3} (1 - \exp(-h\nu_i/kT))^{-1} .$$

The fundamental mode frequencies listed in Reference 12 are used to evaluate $Q_v$.

Equation (9) was obtained by linear regression techniques in an effort to understand the thermal variation of the $NO_2$ absorption coefficient. While the fit to the data is quite good (the linear correlation factor is -0.996 and the F ratio is 101000), this expression is not assumed to have particular theoretical significance. In particular, there is no reason to assume that Eq. (9) can be used for extrapolation to higher temperatures or to wavelengths outside the wavelength range of these measurements.

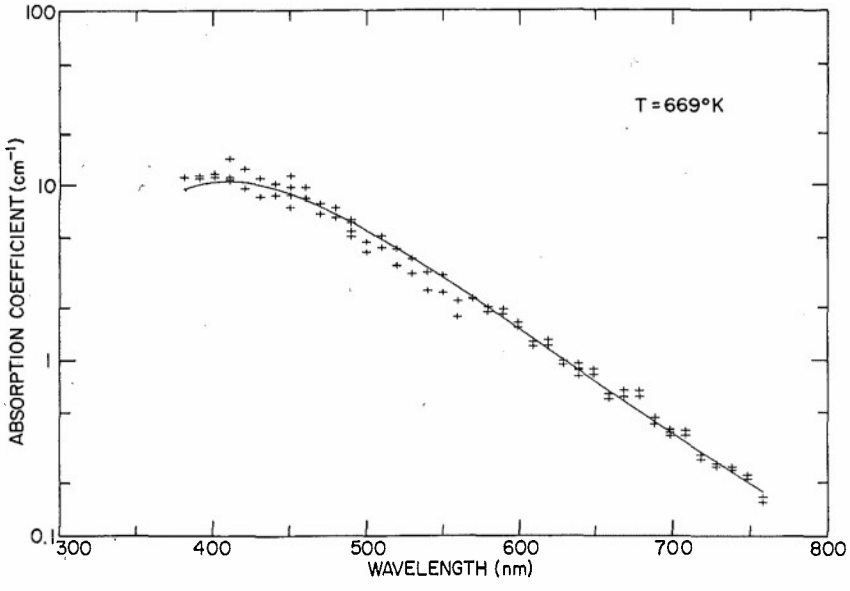


Figure 6. Absorption Coefficient of $NO_2$ as a Function of Wavelength at 669°K

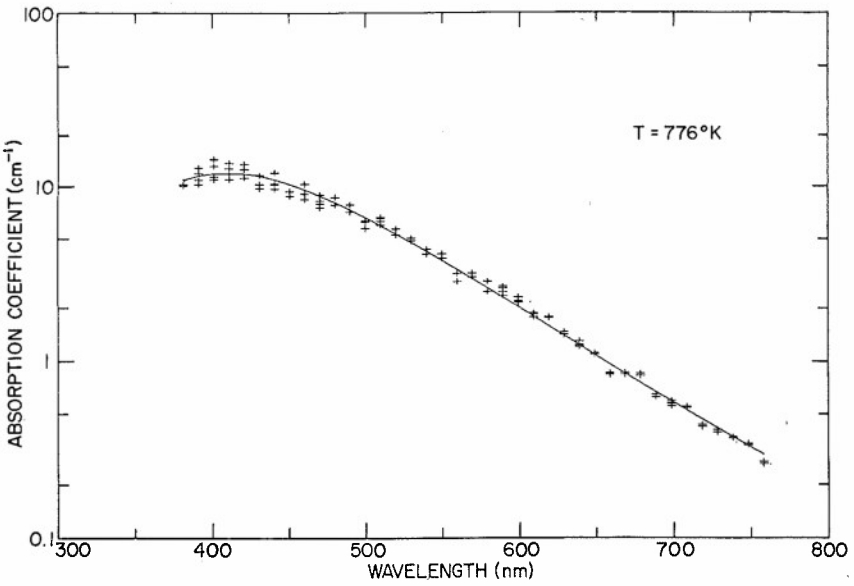


Figure 7. Absorption Coefficient of $NO_2$ as a Function of Wavelength at 776°K

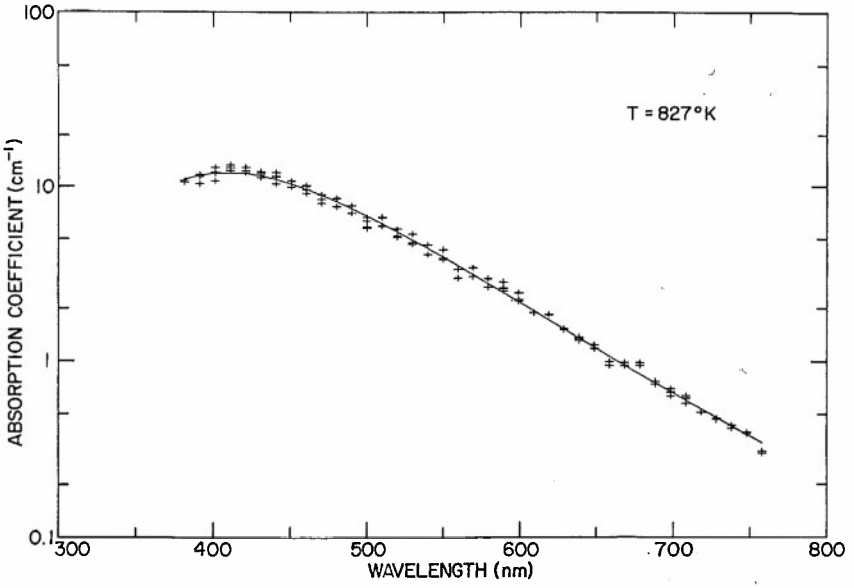


Figure 8. Absorption Coefficient of $NO_2$ as a Function of Wavelength at 827°K

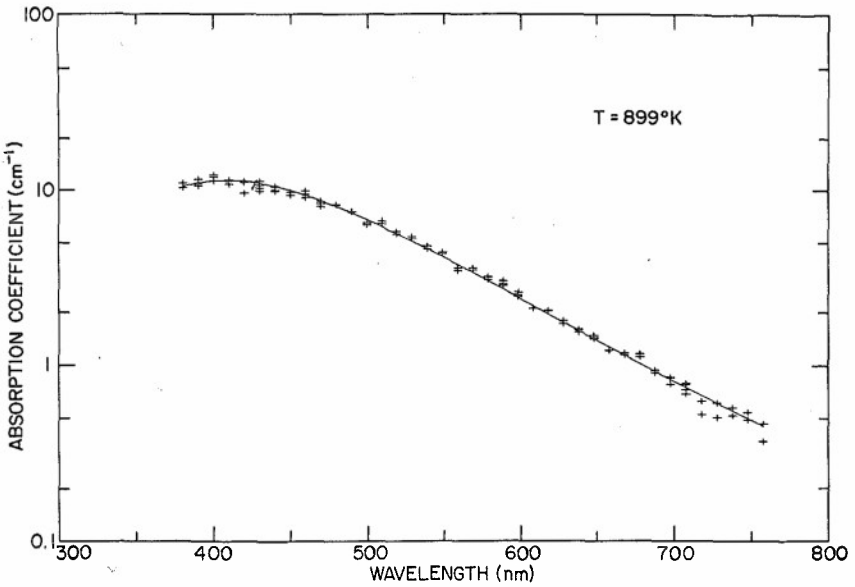


Figure 9. Absorption Coefficient of $NO_2$ as a Function of Wavelength at 899°K

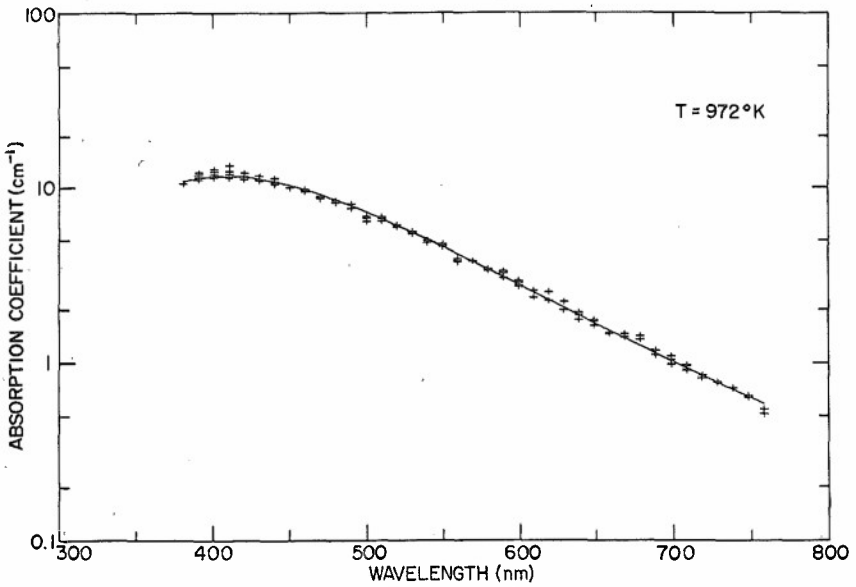


Figure 10. Absorption Coefficient of $NO_2$ as a Function of Wavelength at 972°K

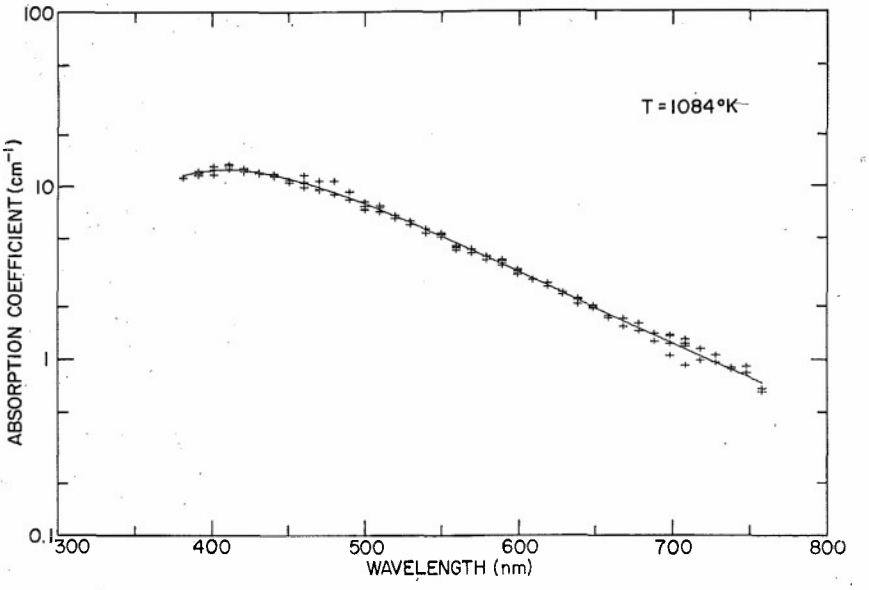


Figure 11. Absorption Coefficient of $NO_2$ as a Function of Wavelength at 1084°K

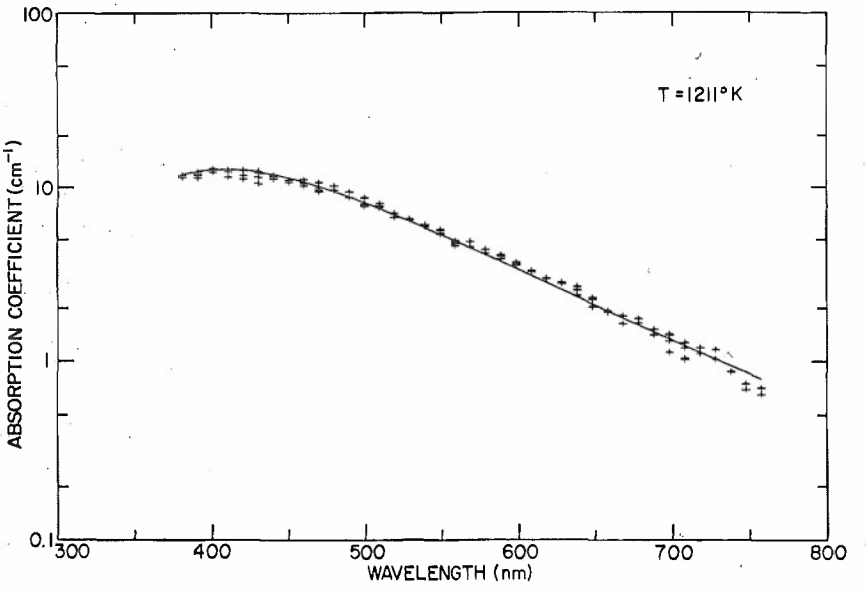


Figure 12. Absorption Coefficient of $NO_2$ as a Function of Wavelength at 1211°K

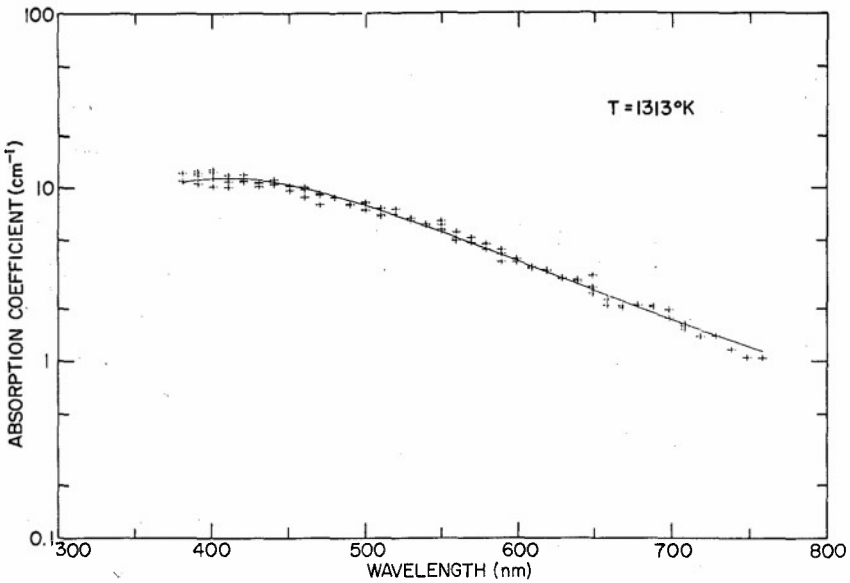


Figure 13. Absorption Coefficient of $NO_2$ as a Function of Wavelength at 1313°K

Table 2a. Mean Absorption Coefficients, Standard Deviations and Number of Data Points as a Function of Temperature and Wavelength ($\bar{T}$ = 669 - 899°K)

| Wavelength (nm) | $\bar{T}$ = 669°K | | | $\bar{T}$ = 776°K | | | $\bar{T}$ = 827°K | | | $\bar{T}$ = 899°K | | |
|---|---|---|---|---|---|---|---|---|---|---|---|---|
| | $\bar{k}$ | $s_k$ | n | $\bar{k}$ | $s_k$ | n | $\bar{k}$ | $s_k$ | n | $\bar{k}$ | $s_k$ | n |
| 380 | 11.95 | 0.01 | 2 | 10.54 | .12 | 2 | 10.87 | .16 | 2 | 11.08 | .49 | 2 |
| 390 | 11.97 | 0.33 | 2 | 11.90 | 1.19 | 4 | 11.50 | .64 | 4 | 11.46 | .44 | 4 |
| 400 | 12.26 | 0.45 | 2 | 12.90 | 1.64 | 4 | 12.15 | .89 | 4 | 12.18 | .46 | 4 |
| 410 | 12.57 | 1.89 | 4 | 12.77 | 1.19 | 4 | 12.96 | .47 | 4 | 11.68 | .29 | 4 |
| 420 | 11.82 | 2.18 | 2 | 12.91 | .95 | 4 | 12.59 | .43 | 4 | 11.20 | .80 | 4 |
| 430 | 10.54 | 1.83 | 2 | 10.85 | .83 | 4 | 12.04 | .41 | 4 | 10.99 | .61 | 4 |
| 440 | 10.19 | 1.12 | 2 | 10.96 | 1.04 | 4 | 11.59 | .73 | 4 | 10.66 | .33 | 4 |
| 450 | 10.04 | 1.77 | 2 | 9.43 | .42 | 2 | 10.61 | .59 | 2 | 9.99 | .28 | 2 |
| 460 | 9.75 | 0.99 | 2 | 9.58 | .82 | 4 | 10.00 | .47 | 4 | 9.91 | .36 | 4 |
| 470 | 7.91 | 0.76 | 2 | 8.50 | .62 | 4 | 8.84 | .48 | 4 | 8.83 | .29 | 4 |
| 480 | 7.51 | 0.66 | 2 | 8.56 | .62 | 2 | 8.33 | .65 | 2 | 8.61 | .01 | 2 |
| 490 | 6.17 | 0.65 | 4 | 7.77 | .52 | 2 | 7.62 | .53 | 2 | 7.87 | .02 | 2 |
| 500 | 4.74 | 0.45 | 2 | 6.36 | .30 | 4 | 6.26 | .41 | 5 | 6.70 | .12 | 4 |
| 510 | 5.09 | 0.57 | 2 | 6.62 | .32 | 4 | 6.42 | .40 | 5 | 6.84 | .17 | 2 |
| 520 | 4.15 | 0.64 | 2 | 5.66 | .33 | 2 | 5.48 | .34 | 3 | 5.93 | .15 | 2 |
| 530 | 3.67 | 0.52 | 2 | 5.11 | .13 | 2 | 5.05 | .38 | 3 | 5.53 | .11 | 2 |
| 540 | 3.00 | 0.52 | 2 | 4.34 | .19 | 2 | 4.35 | .33 | 3 | 4.85 | .14 | 2 |
| 550 | 2.89 | .48 | 2 | 4.09 | .17 | 2 | 4.10 | .30 | 3 | 4.52 | .06 | 2 |
| 560 | 2.16 | .23 | 4 | 3.07 | .24 | 2 | 3.17 | .22 | 3 | 3.61 | .09 | 2 |
| 570 | 2.45 | .17 | 2 | 3.17 | .12 | 2 | 3.29 | .27 | 2 | 3.62 | .07 | 2 |
| 580 | 2.03 | .10 | 2 | 2.72 | .27 | 2 | 2.86 | .23 | 2 | 3.20 | .09 | 2 |
| 590 | 1.97 | .10 | 2 | 2.57 | .14 | 4 | 2.68 | .14 | 4 | 2.97 | .09 | 4 |
| 600 | 1.65 | .08 | 2 | 2.25 | .08 | 4 | 2.32 | .12 | 4 | 2.57 | .08 | 4 |
| 610 | 1.28 | .06 | 2 | 1.85 | .05 | 4 | 1.92 | .00 | 2 | 2.14 | .00 | 2 |
| 620 | 1.30 | .07 | 2 | 1.80 | .02 | 2 | 1.87 | .02 | 2 | 2.08 | .00 | 2 |
| 630 | 1.00 | .04 | 2 | 1.45 | .03 | 2 | 1.54 | .02 | 2 | 1.78 | .05 | 2 |
| 640 | .912 | .064 | 4 | 1.25 | .04 | 4 | 1.36 | .03 | 4 | 1.58 | .03 | 4 |
| 650 | .885 | .049 | 2 | 1.11 | .01 | 2 | 1.21 | .03 | 4 | 1.45 | .03 | 4 |
| 660 | .640 | .030 | 2 | .849 | .015 | 2 | .980 | .034 | 2 | 1.22 | .00 | 2 |
| 670 | .664 | .041 | 2 | .852 | .015 | 2 | .970 | .028 | 2 | 1.16 | .02 | 2 |
| 680 | .664 | .037 | 2 | .840 | .017 | 2 | .971 | .024 | 2 | 1.14 | .03 | 2 |
| 690 | .462 | .028 | 2 | .634 | .017 | 2 | .759 | .019 | 2 | .923 | .023 | 2 |
| 700 | .401 | .016 | 4 | .573 | .017 | 4 | .667 | .026 | 4 | .830 | .037 | 4 |
| 710 | .395 | .018 | 2 | .544 | .005 | 2 | .612 | .026 | 4 | .741 | .047 | 4 |
| 720 | .288 | .012 | 2 | .427 | .008 | 2 | .511 | .001 | 2 | .570 | .070 | 2 |
| 730 | .258 | .007 | 2 | .396 | .010 | 2 | .469 | .006 | 2 | .554 | .076 | 2 |
| 740 | .248 | .008 | 2 | .363 | .004 | 2 | .423 | .013 | 2 | .541 | .041 | 2 |
| 750 | .222 | .008 | 2 | .332 | .004 | 2 | .388 | .004 | 2 | .511 | .035 | 2 |
| 760 | .165 | .008 | 2 | .260 | .006 | 2 | .303 | .006 | 2 | .411 | .068 | 2 |

Table 2b. Mean Absorption Coefficients, Standard Deviations and Number of Data Points as a Function of Temperature and Wavelength ($\bar{T}$ = 972 - 1313°K)

| Wavelength (nm) | $\bar{T}$ = 972°K | | | $\bar{T}$ = 1084°K | | | $\bar{T}$ = 1211°K | | | $\bar{T}$ = 1313°K | | |
|---|---|---|---|---|---|---|---|---|---|---|---|---|
| | $\bar{k}$ | $s_k$ | n | $\bar{k}$ | $s_k$ | n | $\bar{k}$ | $s_k$ | n | $\bar{k}$ | $s_k$ | n |
| 380 | 10.94 | .00 | 2 | 11.38 | .00 | 2 | 11.80 | .22 | 2 | 11.94 | .90 | 2 |
| 390 | 12.12 | .51 | 4 | 12.07 | .32 | 4 | 11.99 | .39 | 4 | 12.13 | .87 | 4 |
| 400 | 12.58 | .62 | 4 | 12.59 | .57 | 4 | 12.72 | .25 | 4 | 12.03 | 1.19 | 4 |
| 410 | 12.84 | .91 | 4 | 13.26 | .40 | 4 | 12.51 | .56 | 4 | 11.38 | .78 | 4 |
| 420 | 12.03 | .49 | 4 | 12.70 | .28 | 4 | 12.24 | .67 | 4 | 11.55 | .49 | 4 |
| 430 | 11.68 | .37 | 4 | 12.15 | .13 | 4 | 11.89 | .84 | 4 | 10.91 | .29 | 4 |
| 440 | 11.28 | .42 | 4 | 11.83 | .18 | 4 | 11.74 | .28 | 4 | 11.03 | .32 | 4 |
| 450 | 10.44 | .04 | 2 | 10.91 | .27 | 2 | 11.13 | .21 | 2 | 10.29 | .44 | 2 |
| 460 | 10.05 | .14 | 4 | 10.82 | .74 | 4 | 10.88 | .38 | 4 | 10.02 | .60 | 4 |
| 470 | 9.09 | .12 | 4 | 10.07 | .59 | 4 | 10.19 | .54 | 4 | 9.20 | .64 | 4 |
| 480 | 8.64 | .20 | 2 | 10.05 | 1.25 | 2 | 10.15 | .40 | 2 | 9.11 | .02 | 2 |
| 490 | 8.13 | .31 | 2 | 8.99 | .67 | 2 | 9.29 | .49 | 2 | 8.27 | .07 | 2 |
| 500 | 6.93 | .20 | 4 | 7.72 | .39 | 4 | 8.29 | .44 | 4 | 8.08 | .46 | 4 |
| 510 | 6.88 | .16 | 4 | 7.48 | .28 | 4 | 7.96 | .21 | 4 | 7.49 | .43 | 4 |
| 520 | 6.25 | .12 | 2 | 6.76 | .21 | 2 | 7.04 | .28 | 2 | 7.52 | .40 | 2 |
| 530 | 5.69 | .11 | 2 | 6.20 | .20 | 2 | 6.65 | .03 | 2 | 6.78 | .17 | 2 |
| 540 | 5.07 | .10 | 2 | 5.59 | .24 | 2 | 6.15 | .10 | 2 | 6.30 | .09 | 2 |
| 550 | 4.81 | .07 | 4 | 5.30 | .11 | 5 | 5.64 | .16 | 4 | 6.14 | .38 | 4 |
| 560 | 3.92 | .07 | 4 | 4.44 | .10 | 5 | 4.84 | .14 | 4 | 5.28 | .28 | 4 |
| 570 | 3.90 | .00 | 2 | 4.27 | .13 | 3 | 4.76 | .25 | 2 | 5.10 | .25 | 2 |
| 580 | 3.47 | .06 | 2 | 3.89 | .11 | 3 | 4.32 | .16 | 2 | 4.66 | .25 | 2 |
| 590 | 3.29 | .12 | 4 | 3.65 | .11 | 5 | 4.03 | .09 | 4 | 4.19 | .29 | 4 |
| 600 | 2.87 | .10 | 4 | 3.21 | .10 | 5 | 3.63 | .06 | 4 | 3.90 | .08 | 4 |
| 610 | 2.52 | .16 | 2 | 2.88 | .01 | 2 | 3.29 | .04 | 2 | 3.53 | .05 | 2 |
| 620 | 2.44 | .21 | 2 | 2.68 | .08 | 2 | 2.99 | .00 | 2 | 3.38 | .04 | 2 |
| 630 | 2.14 | .17 | 2 | 2.40 | .04 | 2 | 2.81 | .03 | 2 | 3.04 | .04 | 2 |
| 640 | 1.89 | .09 | 4 | 2.18 | .08 | 4 | 2.55 | .12 | 4 | 2.93 | .05 | 4 |
| 650 | 1.73 | .06 | 4 | 1.99 | .04 | 4 | 2.23 | .12 | 4 | 2.75 | .30 | 4 |
| 660 | 1.47 | .00 | 2 | 1.73 | .03 | 2 | 1.93 | .03 | 2 | 2.21 | .12 | 2 |
| 670 | 1.44 | .04 | 2 | 1.61 | .13 | 2 | 1.73 | .13 | 2 | 2.08 | .04 | 2 |
| 680 | 1.40 | .05 | 2 | 1.52 | .11 | 2 | 1.71 | .07 | 2 | 2.12 | .01 | 2 |
| 690 | 1.15 | .05 | 2 | 1.32 | .10 | 2 | 1.47 | .07 | 2 | 2.08 | .03 | 2 |
| 700 | 1.03 | .06 | 4 | 1.24 | .15 | 4 | 1.32 | .14 | 4 | 1.85 | .13 | 3 |
| 710 | .938 | .033 | 4 | 1.15 | .17 | 4 | 1.13 | .12 | 4 | 1.59 | .06 | 3 |
| 720 | .834 | .023 | 2 | 1.05 | .11 | 2 | 1.15 | .06 | 2 | 1.39 | — | 1 |
| 730 | .773 | .006 | 2 | .995 | .070 | 2 | 1.10 | .10 | 2 | 1.41 | — | 1 |
| 740 | .714 | .003 | 2 | .875 | .016 | 2 | .871 | .004 | 2 | 1.17 | — | 1 |
| 750 | .637 | .011 | 2 | .859 | .054 | 2 | .713 | .036 | 2 | 1.05 | — | 1 |
| 760 | .524 | .023 | 2 | .654 | .021 | 2 | .674 | .040 | 2 | 1.04 | — | 1 |

## 4. DISCUSSION

The precision of the measurements is about 5 percent, which is the typical standard deviation of the absorption coefficient at a given wavelength and temperature. It is difficult to assess the accuracy of these measurements. Total pressure is known to better than 2 percent. Photocurrents are typically measured to about 1 percent accuracy. The temperatures are measured to ±3°K.

The determination of the pressure of $NO_2$ in the absorption cell is the main source of inaccuracy. The thermochemical data[12] should be quite accurate. The calculated $NO_2$ pressure, under isothermal conditions, would probably be accurate to ±2 or 3 percent. However, part of the system is at low temperatures and this introduces the perturbation to equilibrium which is described in the previous section. We believe that the empirical approach to this problem has reduced the inaccuracy of the cross-sections to ±10 percent. A comparison of our data to the previously published absorption coefficients (see Figure 1) shows that the present results lie close to or a little below the previously published data. The discrepancies lie within the experimental uncertainties of the measurements.

These results therefore support the previous data and provide more detailed information. They do not provide absorption coefficients for $NO_2$ at temperatures beyond about 1500°K.

At higher temperatures, it is not recommended that emission intensities from shock tube[3] or other experiments[1] be converted into the corresponding absorption coefficients for $NO_2$. As shown in Figure 1, absorption coefficients which are calculated from shock tube emission intensities are considerably different from the measured absorption coefficients for $NO_2$. We have also calculated the absorption coefficients from the emission intensities obtained with the same equipment;[1] the results were similar to those shown by Gilmore.[2]

These results are considered to be only an apparent contradiction of Kirchoff's Law. It has been known for some time[13, 14] that the radiative transitions of $NO_2$ exhibit "anomalous" behavior. For example, the fluorescent radiative lifetimes for $NO_2$ are much longer than that which is calculated from the integrated absorption coefficient. The molecule is a relatively complex system, with a bent ground state and several linear and bent excited states 2 to 3 eV above the ground state. The exact configurations of these excited states are largely unknown. Due to the variety of possible interactions, perturbations, radiationless transitions, etc., that can take place it is not surprising that anomalous results are observed.

13. Neuberger, D. and Duncan, A.E.F. (1954) J. Chem. Phys. 22:1963.
14. Douglas, A.E. (1966) J. Chem. Phys. 45:1007.

The system is complicated enough so that the related emission and absorption processes cannot be isolated in the observed spectra, and therefore an application of Kirchoff's Law appears to be not readily possible. The separate measurement in the same laboratory of the thermal emission[1] and the absorption coefficient reported here should amply demonstrate this situation. Therefore, it is recommended that computer codes not convert emission data to absorption data and vice-versa for the $NO_2$ molecule, since the present results, coupled with earlier measurements, demonstrate errors in this technique. If absorption coefficients are required, only measured values should be used.

## References


1. Paulsen, D.E., Sheridan, W.F., and Huffman, R.E. (1970) J. Chem. Phys. 53:647.
2. Gilmore, F.R. (1965) J. Quant. Spectry. Radiative Transfer 5:125 and references therein.
3. Levitt, B.P. (1965) J. Chem. Phys. 42:1038.
4. Dixon, J.K. (1940) J. Chem. Phys. 8:157.
5. Hall, T.C. and Blacet, F.E. (1952) J. Chem. Phys. 20:1745.
6. Heath, D.F. and Dieke, G.H. (1957) Absorption of $NO_2$, unpublished, included in Reference 2.
7. Schott, G. and Davidson, N. (1958) J. Am. Chem. Soc. 80:1841.
8. Huffman, R.E. and Davidson, N. (1959) J. Am. Chem. Soc. 81:2311.
9. Nakayama, T., Kitamura, M., and Watanabe, K. (1959) J. Chem. Phys. 30:1180.
10. Wurster, W.H. and Marrone, P.V. (1961) Study of Infrared Emission in Heated Air, QM-1373-A-4, Cornell Aeronautical Laboratory, Buffalo, New York.
11. Levitt, B.P. (1962) Trans. Faraday Soc. 58:1789.
12. JANAF Thermochemical Tables, (1965) Dow Chemical, Midland, Michigan.
13. Neuberger, D. and Duncan, A.E.F. (1954) J. Chem. Phys. 22:1963.
14. Douglas, A.E. (1966) J. Chem. Phys. 45:1007.

## DISTRIBUTION LIST

ASSISTANT TO THE SECRETARY OF DEFENSE
ATOMIC ENERGY
DEPARTMENT OF DEFENSE
WASHINGTON DC 20301
1 01CY ATTN HONORABLE DONALD R COTTER

DIRECTOR
DEFENSE ADVANCED RSCH PROJ AGENCY
ARCHITECT BUILDING
1400 WILSON BLVD.
ARLINGTON, VA 22209
01CY ATTN MAJOR GREGORY CANAVAN
01CY ATTN LTC W A WHITAKER
01CY ATTN ROBERT A MOORE
01CY ATTN STO CAPT J JUSTICE
01CY ATTN TIO FRED A KOETHER

DEFENSE DOCUMENTATION CENTER
CAMERON STATION
ALEXANDRIA, VA 22314
(12 COPIES IF OPEN PUBLICATION,
12CY ATTN TC

DIRECTOR
DEFENSE NUCLEAR AGENCY
WASHINGTON, DC 20305
01CY ATTN RAAE HAROLD C FITZ JR
03CY ATTN STTL TECH LIBRARY
01CY ATTN STSI ARCHIVES
01CY ATTN DDST
01CY ATTN RAAE CHARLES A BLANK
01CY ATTN RAAE MAJ JOHN CLARK
01CY ATTN RAAE P FLEMING

DIR OF DEFENSE RSCH & ENGINEERING
DEPARTMENT OF DEFENSE
WASHINGTON DC 20301
01CY ATTN DD/S&SS DANIEL BROCKWAY
01CY ATTN DDS&SS RICHARD S RUFFINE
01CY ATTN JAMES P WADE

COMMANDER
FIELD COMMAND
DEFENSE NUCLEAR AGENCY
KIRTLAND AFB, NM 87115
01CY ATTN FCPR

CHIEF
LIVERMORE DIVISION FLD COMMAND DNA
LAWRENCE LIVERMORE LABORATORY
P.O. BOX 808
LIVERMORE, CA 94550
01CY ATTN FCPRL

COMMANDER/DIRECTOR
ATMOSPHERIC SCIENCES LABORATORY
U S ARMY ELECTRONICS COMMAND
WHITE SANDS MISSILE RANGE, NM 88002
01CY ATTN E BUTTERFIELD DRSEL-BL-SY-R
01CY ATTN DRSSEL-BL-SY-S F E NILES

DIRECTOR
BMD ADVANCED TECH CTR
HUNTSVILLE OFFICE
P.O. BOX 1500
HUNTSVILLE, AL 35807
01CY ATTN ATC-T MELVIN T CAPPS
01CY ATTN CRDABH-D W DAVIES

PROGRAM MANAGER
BMD PROGRAM OFFICE
1300 WILSON BLVD
ARLINGTON VA 22209
01CY ATTN DACS-BMM

COMMANDER
HARRY DIAMOND LABORATORIES
2800 POWDER MILL ROAD
ADELPHI MD 20783
02CY ATTN DRXDO-NP
01CY ATTN DRXDO-TI TECH LIB

COMMANDER
U S ARMY MATERIEL DEV & READINESS CMD
5001 EISENHOWER AVENUE
ALEXANDRIA, VA 22333
01CY ATTN DRCLDC J A BENDER

COMMANDER
U S ARMY NUCLEAR AGENCY
FORT BLISS, TX 79916
01CY ATTN ATCA-NAW J BERBERET

CHIEF OF NAVAL OPERATIONS
NAVY DEPARTMENT
WASHINGTON, DC 20350
01CY ATTN OP 985

CHIEF OF NAVAL RESEARCH
NAVY DEPARTMENT
ARLINGTON, VA 22217
01CY ATTN CODE 464 R GRACEN JOINER
01CY ATTN CODE 464 THOMAS P QUINN

COMMANDER
NAVAL ELECTRONICS LABORATORY CENTER
SAN DIEGO, CA 92152
01CY ATTN CODE 2200 ILAN ROTHMULLER

DIRECTOR
NAVAL RESEARCH LABORATORY
WASHINGTON, DC 20375
01CY ATTN CODE 7127 CHARLES Y JOHNSON
01CY ATTN CODE 7700 TIMOTHY P COFFEY
01CY ATTN CODE 7701 JACK D BROWN
01CY ATTN CODE 7750 WAHAB ALI
01CY ATTN CODE 7750 S L OSSAKOW

COMMANDER
NAVAL SURFACE WEAPONS CENTER
WHITE OAK, SILVER SPRING, MD 20910
01CY ATTN CODE WA501 NAVY NUC PRGMS OF

AF GEOPHYSICS LABORATORY, AFSC
HANSCOM AFB, MA 01731
01CY ATTN OPR HAROLD GARDNER
01CY ATTN LKB KENNETH S W CHAMPION
01CY ATTN OPR JAMES C ULWICK
01CY ATTN LKB JOHN PAULSON
01CY ATTN OPR ALVA T STAIR
01CY ATTN LKD ROCCO S NARCISI
02CY ATTN LKD ROBERT E HUFFMAN
01CY ATTN OP JOHN S GARING

HQ USAF/RD
WASHINGTON, DC 20330
01CY ATTN RDQPN
01CY ATTN RDQ

SAMSO/AW
P.O. BOX 92960
WORLDWAY POSTAL CENTER
LOS ANGELES, CA 90009
03CY ATTN AWW

SAMSO/SZ
POST OFFICE BOX 92960
WORLDWAY POSTAL CENTER
LOS ANGELES, CA 90009
(SPACE DEFENSE SYSTEMS)
01CY ATTN SZJ MAJOR LAWRENCE DOAN

USAFETAC/CB
SCOTT AFB IL 62225
01CY ATTN CBT MR CREASI

DIVISION OF MILITARY APPLICATION
U S ENERGY RSCH & DEV ADMIN
WASHINGTON, DC 20545
01CY ATTN DOC CON FOR MAJ D A HAYCOCK

LOS ALAMOS SCIENTIFIC LABORATORY
P.O. BOX 1663
LOS ALAMOS, NM 87545
01CY ATTN DOC CON FOR JOHN S MALIK
01CY ATTN DOC CON FOR R A JEFFRIES

AEROSPACE CORPORATION
P.O. BOX 92957
LOS ANGELES, CA 90009
01CY ATTN T TAYLOR
01CY ATTN HARRIS MAYER

GENERAL ELECTRIC COMPANY
SPACE DIVISION
VALLEY FORGE SPACE CENTER
GODDARD BLVD KING OF PRUSSIA
P.O. BOX 8555
PHILADELPHIA PA 19101
01CY ATTN T BAUER
01CY ATTN M H BORTNER SPACE SCI LAB

GENERAL ELECTRIC COMPANY
TEMPO-CENTER FOR ADVANCED STUDIES
816 STATE STREET (P.O. DRAWER QQ)
SANTA BARBARA, CA 93102
01CY ATTN TIM STEPHENS
01CY ATTN DASIAC
01CY ATTN WARREN S KNAPP

GENERAL RESEARCH CORPORATION
P.O. BOX 3587
SANTA BARBARA, CA 93105
01CY ATTN JOHN ISE JR

INSTITUTE FOR DEFENSE ANALYSES
400 ARMY-NAVY DRIVE
ARLINGTON, VA 22202
01CY ATTN HANS WOLFHARD
01CY ATTN ERNEST BAUER
01CY ATTN JOEL BENGSTON

LOCKHEED MISSILES AND SPACE COMPANY
3251 HANOVER STREET
PALO ALTO, CA 94304
01CY ATTN MARTIN WALT DEPT 52-10
01CY ATTN BILLY M MCCORMAC DEPT 52-14
01CY ATTN ROBERT D SEARS DEPT 52-14

M.I.T. LINCOLN LABORATORY
P.O. BOX 73
LEXINGTON, MA 02173
01CY ATTN LIB A-082 FOR DAVID M TOWLE

MISSION RESEARCH CORPORATION
735 STATE STREET
SANTA BARBARA, CA 93101
01CY ATTN P FISCHER
01CY ATTN D SAPPENFIELD
01CY ATTN M SCHEIBE
01CY ATTN DAVE SOWLE
01CY ATTN R HENDRICK

PHOTOMETRICS, INC.
442 MARRETT ROAD
LEXINGTON, MA 02173
03CY ATTN IRVING L KOFSKY

PHYSICAL DYNAMICS INC.
P.O. BOX 1069
BERKELEY, CA 94701
01CY ATTN A THOMPSON

PHYSICAL SCIENCES, INC.
30 COMMERCE WAY
WOBURN, MA 01801
01CY ATTN KURT WRAY

R & D ASSOCIATES
P.O. BOX 9695
MARINA DEL REY CA 90291
01CY ATTN FORREST GILMORE
01CY ATTN ROBERT F LELEVIER

R & D ASSOCIATES
1815 N. FT. MYER DRIVE
11TH FLOOR
ARLINGTON, VA 22209
01CY ATTN HERBERT J MITCHELL

SCIENCE APPLICATIONS, INC.
P.O. BOX 2351
LA JOLLA, CA 92038
01CY ATTN DANIEL A HAMLIN

STANFORD RESEARCH INSTITUTE
333 RAVENSWOOD AVENUE
MENLO PARK, CA 94025
01CY ATTN VINCENT L WICKWAR
01CY ATTN RAY L LEADABRAND

STANFORD RESEARCH INSTITUTE
1611 NORTH KENT STREET
ARLINGTON, VA 22209
01CY ATTN WARREN W BERNING

VISIDYNE, INC.
19 THIRD AVENUE
NORTH WEST INDUSTRIAL PARK
BURLINGTON, MA 01803
01CY ATTN HENRY J SMITH
01CY ATTN J W CARPENTER
01CY ATTN WILLIAM REIDY